Supplementary Materials for

Unraveling the Deactivation Mechanism and Stability Enhancement of Cobalt-based Heterogenous Co_3O_4/g-C_3N_4 Catalysts in CO_2 Hydrogenation

The PDF file includes:

Figs. S1 to S23

Tab. S1

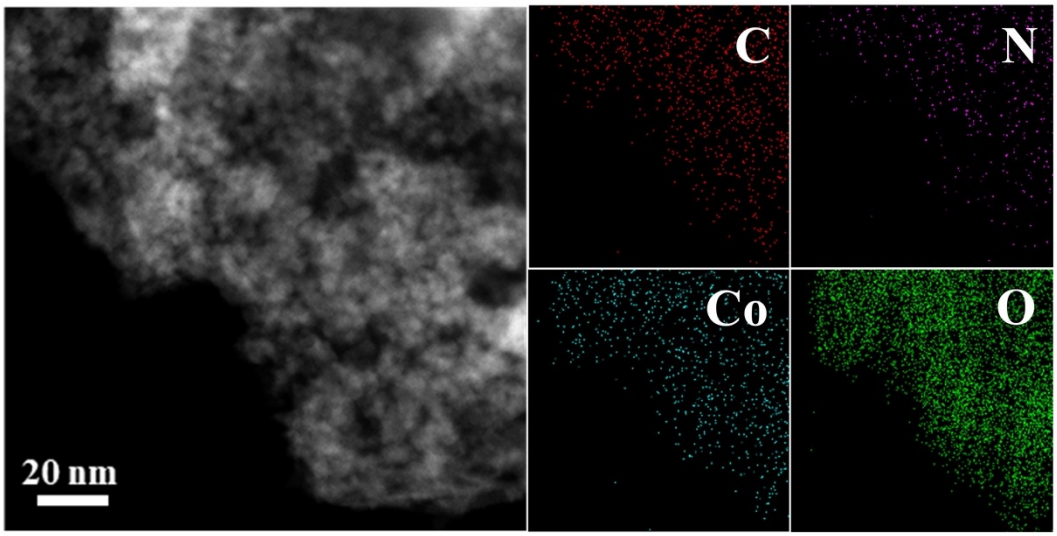

Figure S1. EDS mapping of Co_3O_4/g-C_3N_4-10.

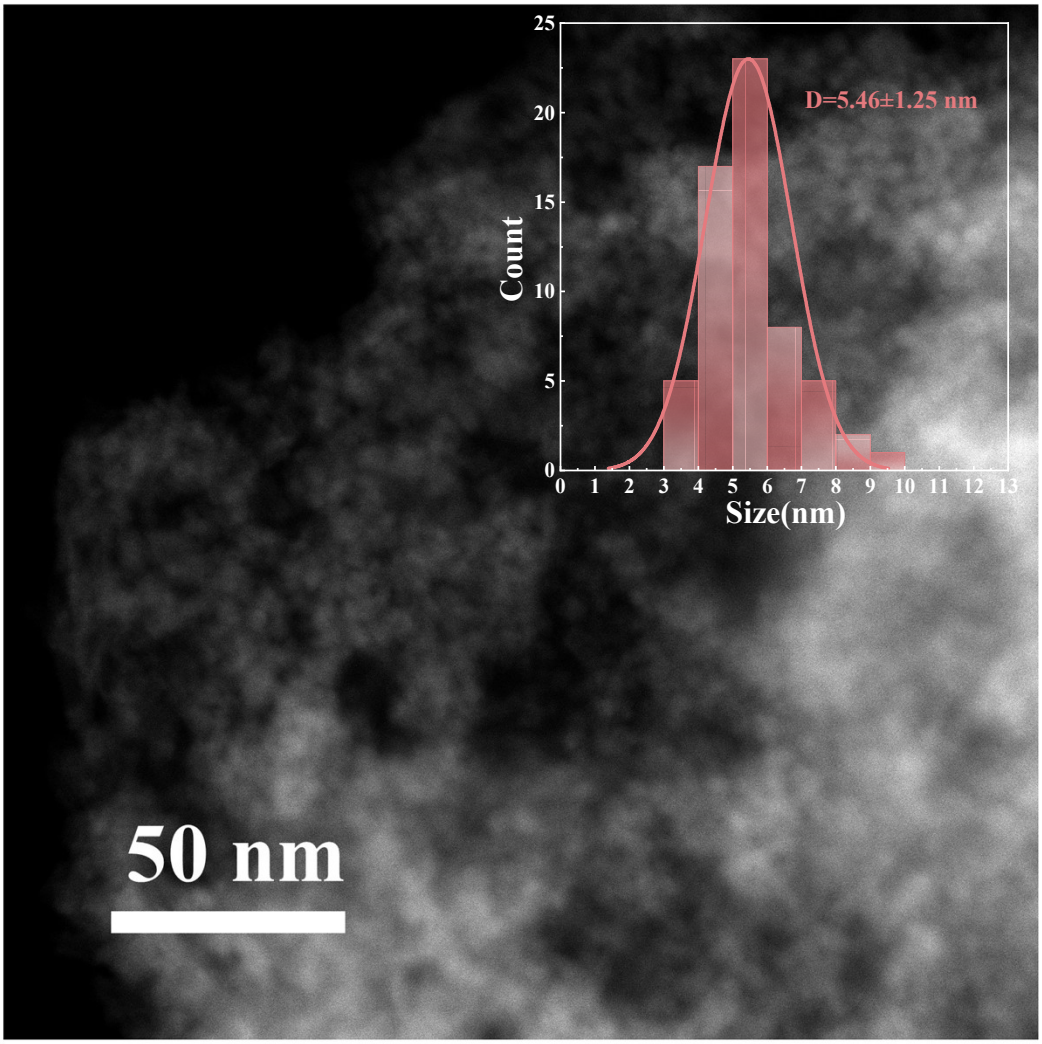

Figure S2. Particle size distribution of Co_3O_4/g-C_3N_4-10.

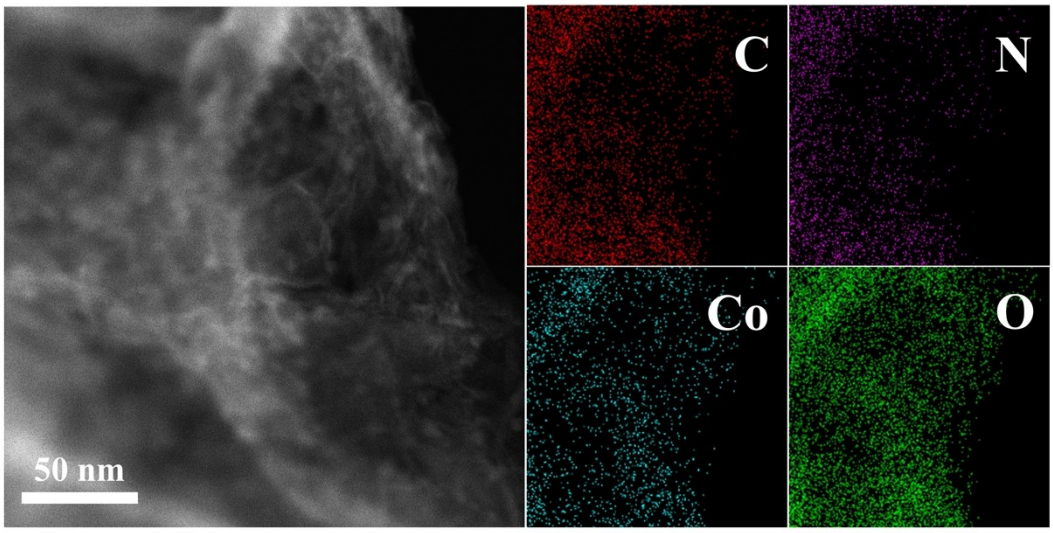

Figure S3. EDS mapping of Co_3O_4/g-C_3N_4-50.

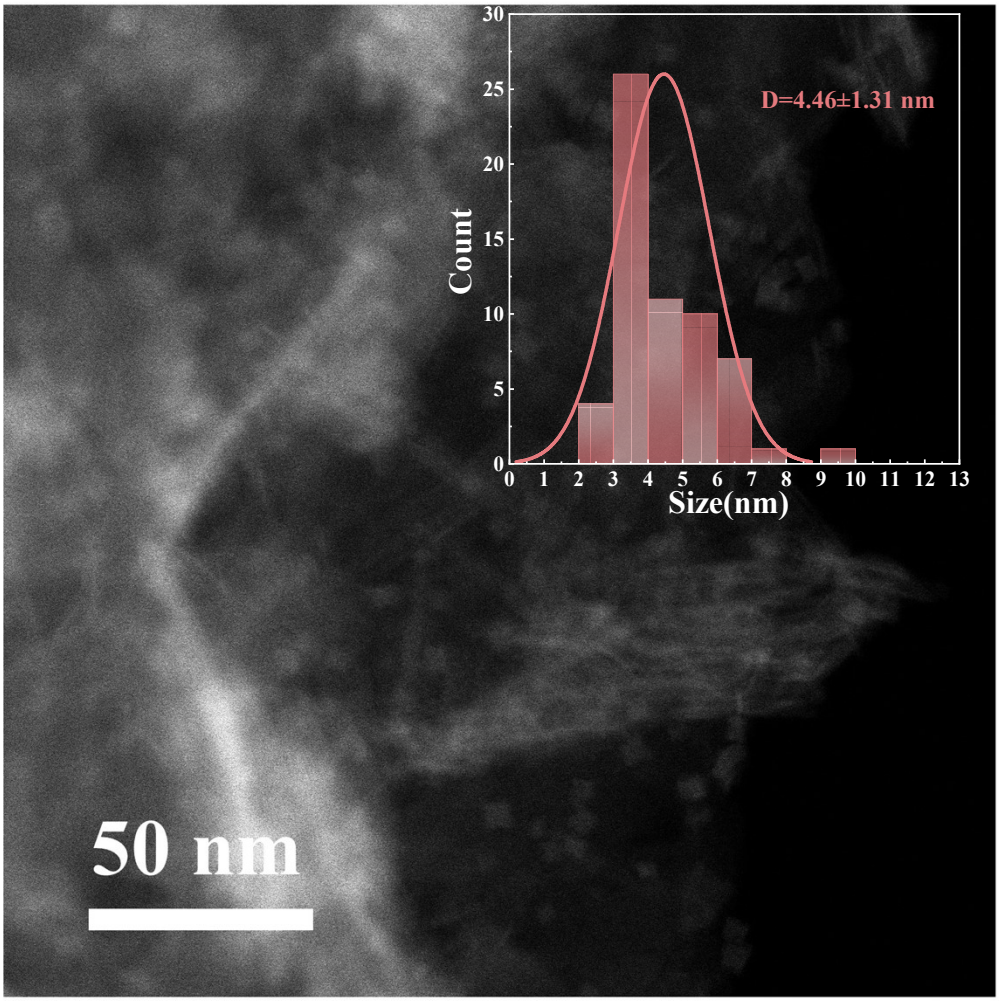

Figure S4. Particle size distribution of Co_3O_4/g-C_3N_4-50.

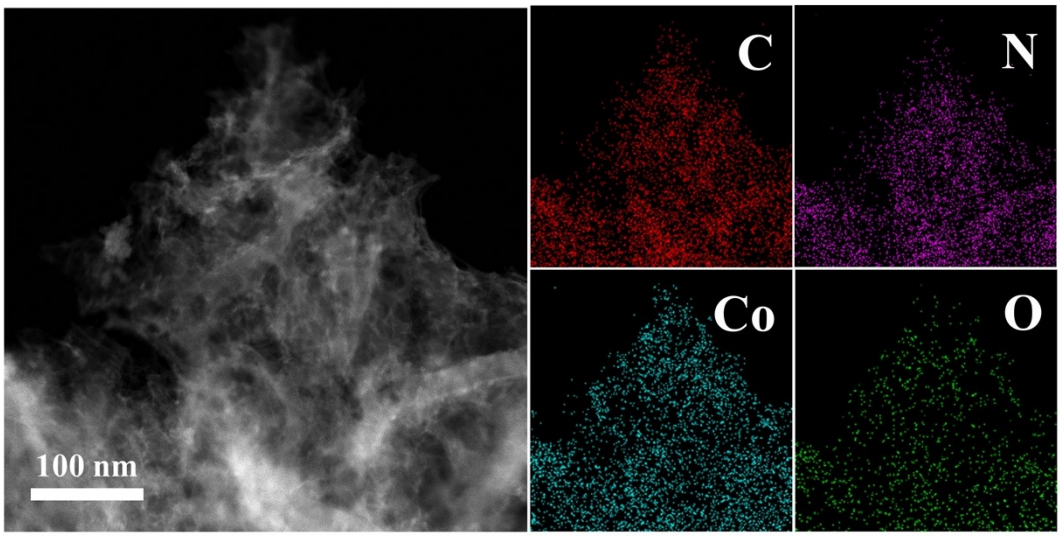

Figure S5. EDS mapping of Co_3O_4/g-C_3N_4-90.

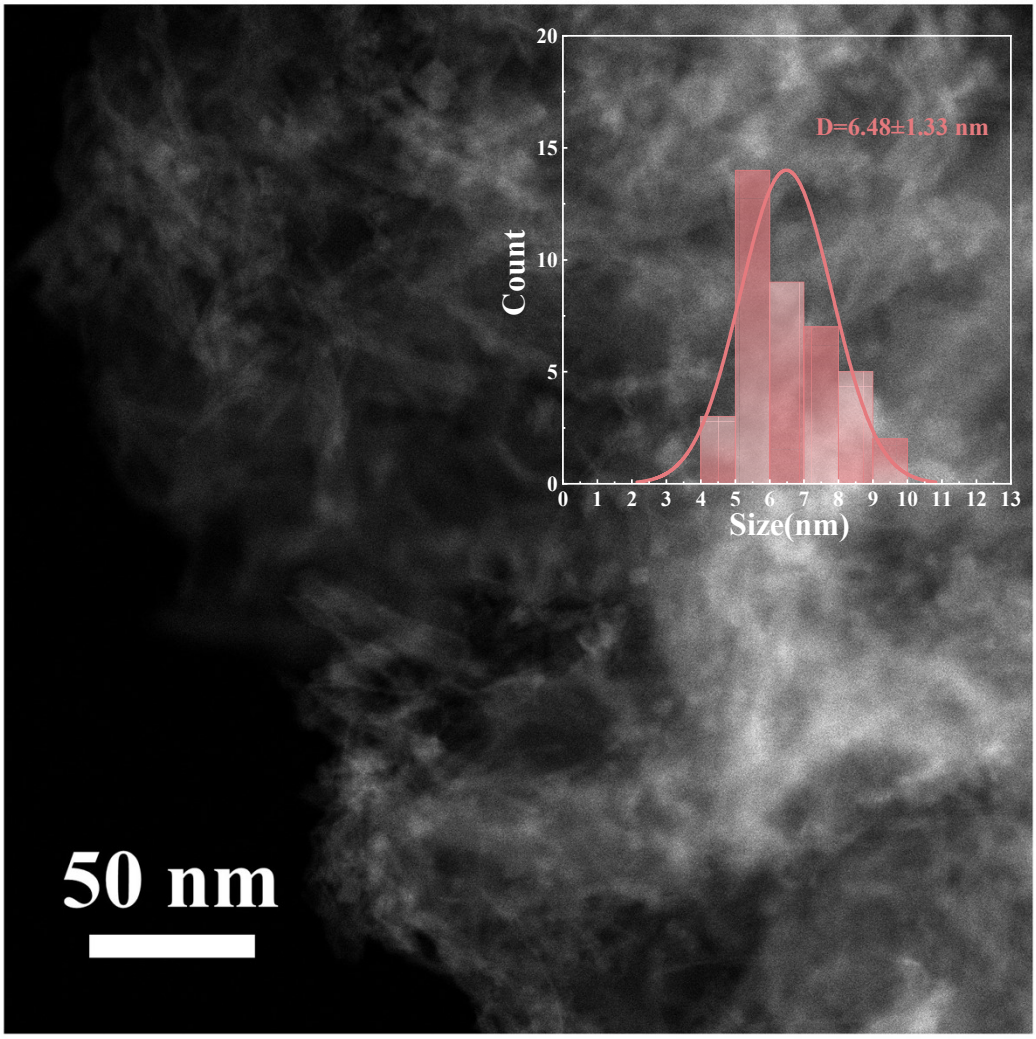

Figure S6. Particle size distribution of Co_3O_4/g-C_3N_4-90.

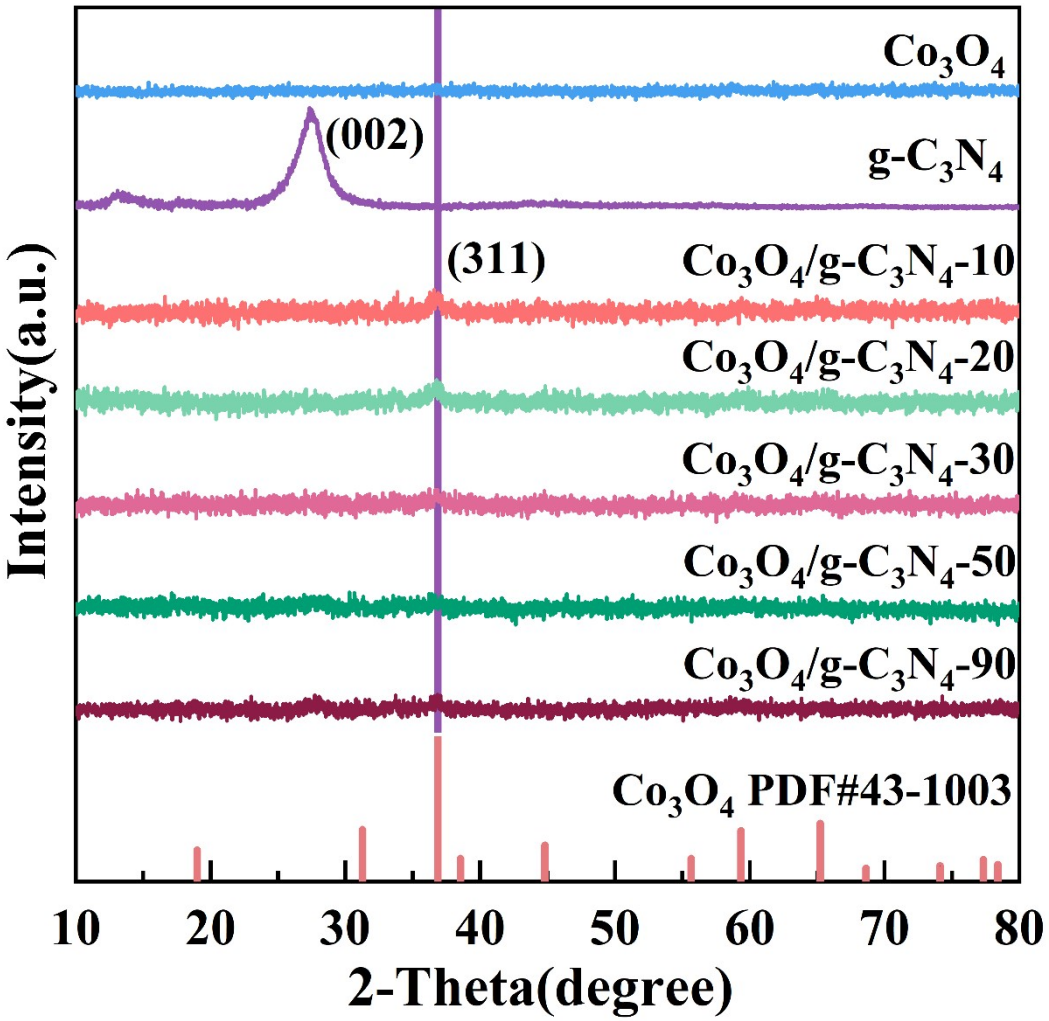

Fig. S7 XRD patterns of catalysts with different g-C_3N_4 loadings.

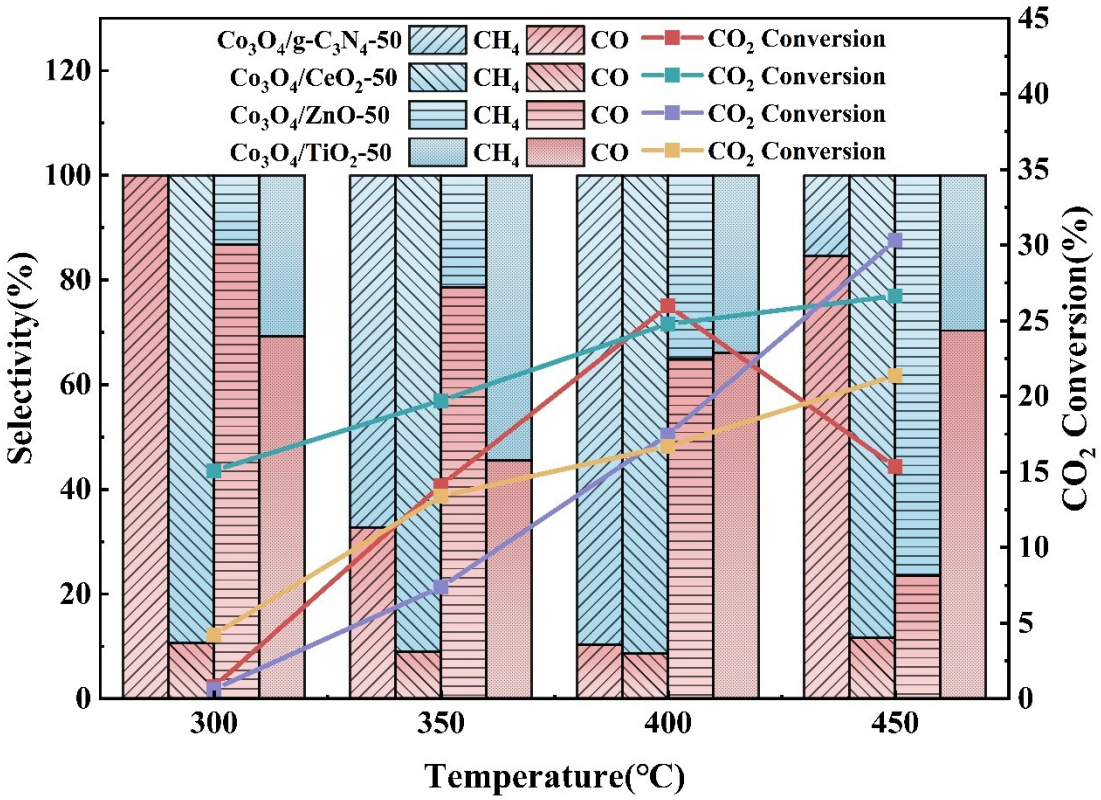

Figure S8. Catalytic performance of Co_3O_4 supported on g-C_3N_4, CeO_2, ZnO and TiO_2 at different temperatures.

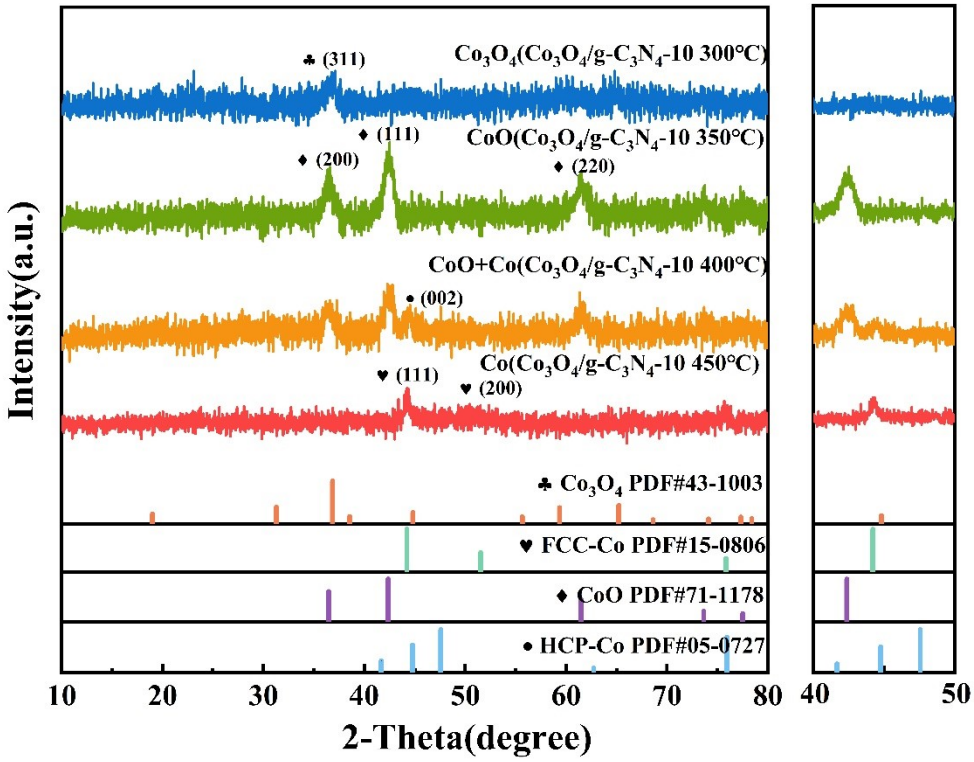

Figure S9. XRD of Co_3O_4/g-C_3N_4-10 at different reaction temperatures.

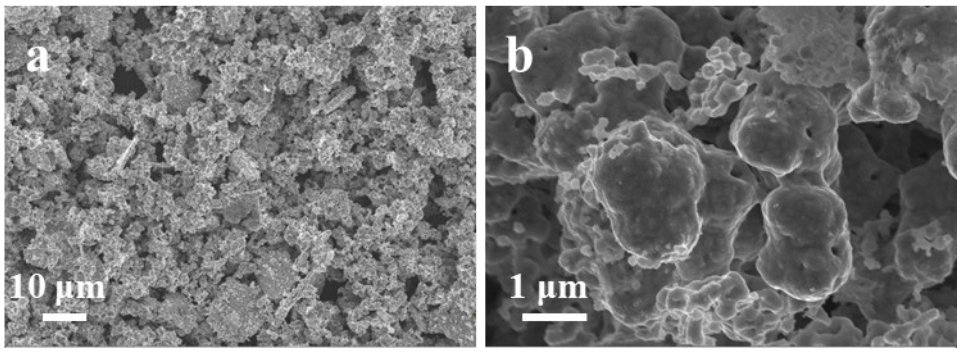

Figure S10. SEM image of the Co_3O_4 NPs after 20 h cycling stability at 450 ℃

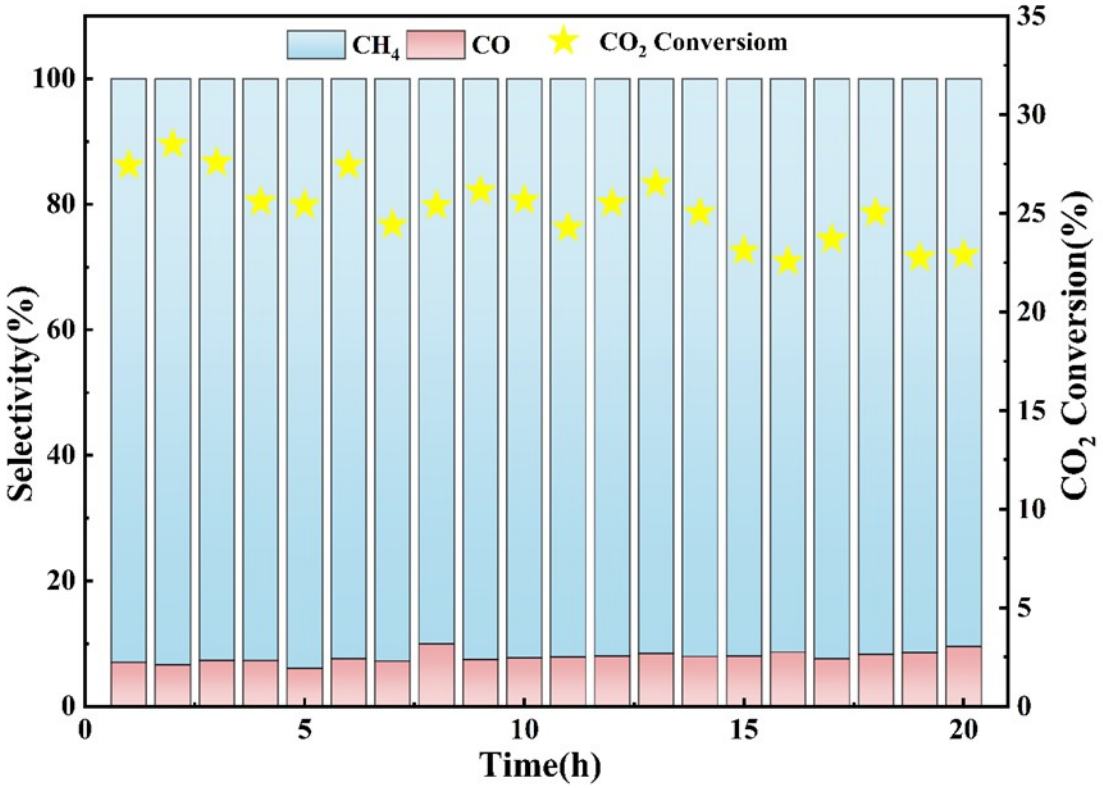

Figure S11. Cycling stability of Co_3O_4 NPs at 350 ℃ over 20 h.

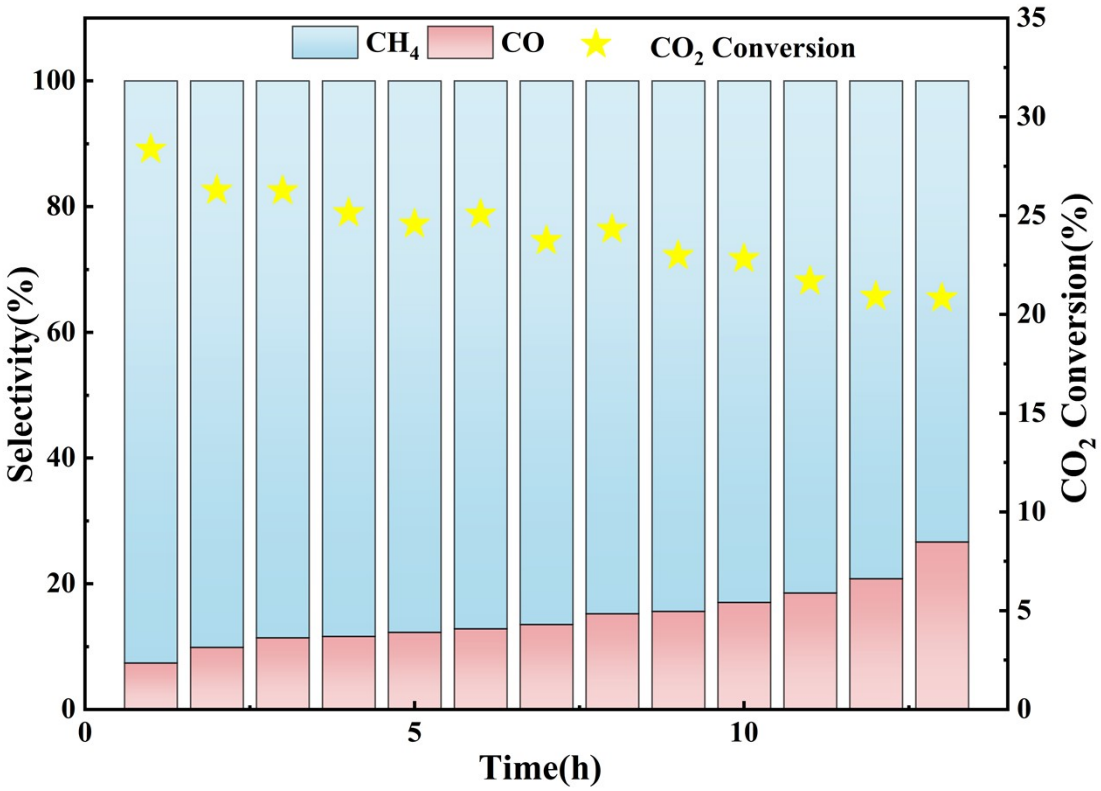

Figure S12. Cycling stability of Co_3O_4/g-C_3N_4-10 at 400 ℃ over 13 h.

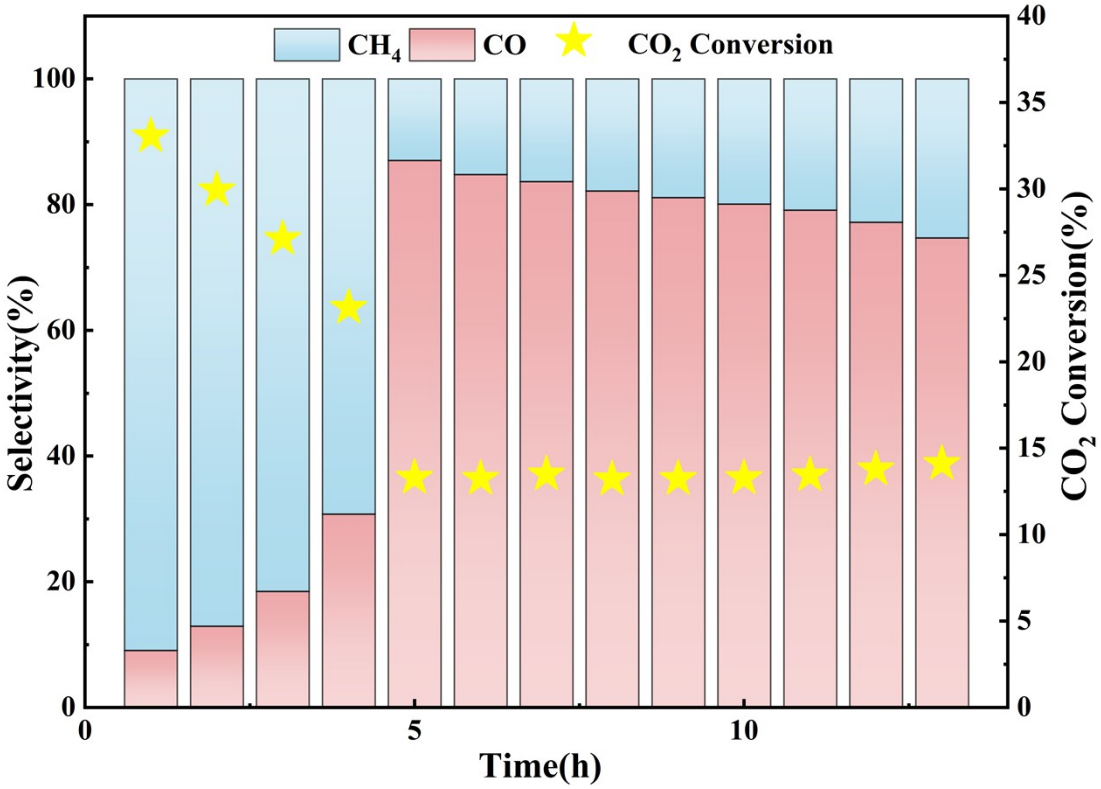

Figure S13. Cycling stability of Co_3O_4/g-C_3N_4-20 at 400 ℃ over 13 h.

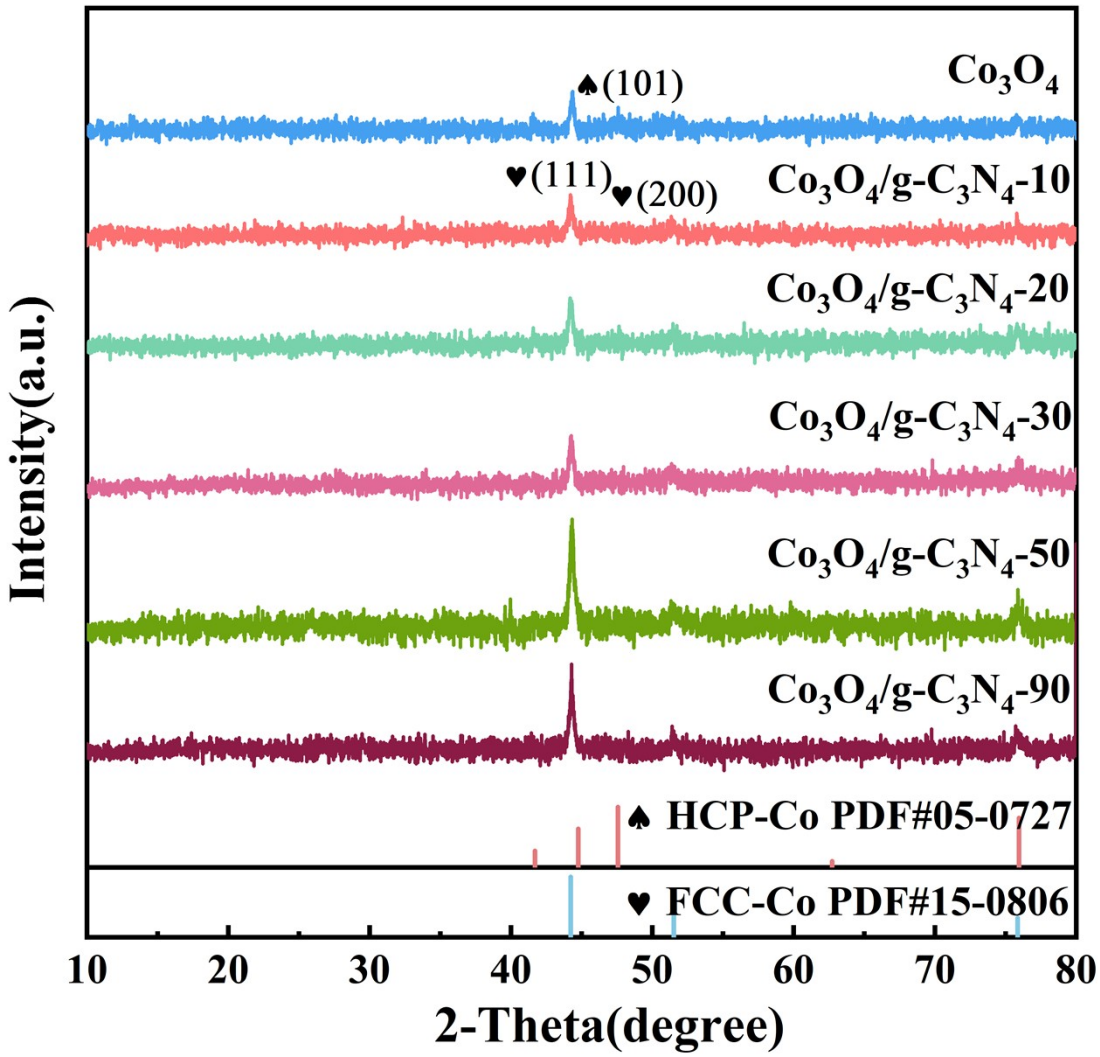

Figure S14. XRD patterns of the catalyst after performance evaluation.

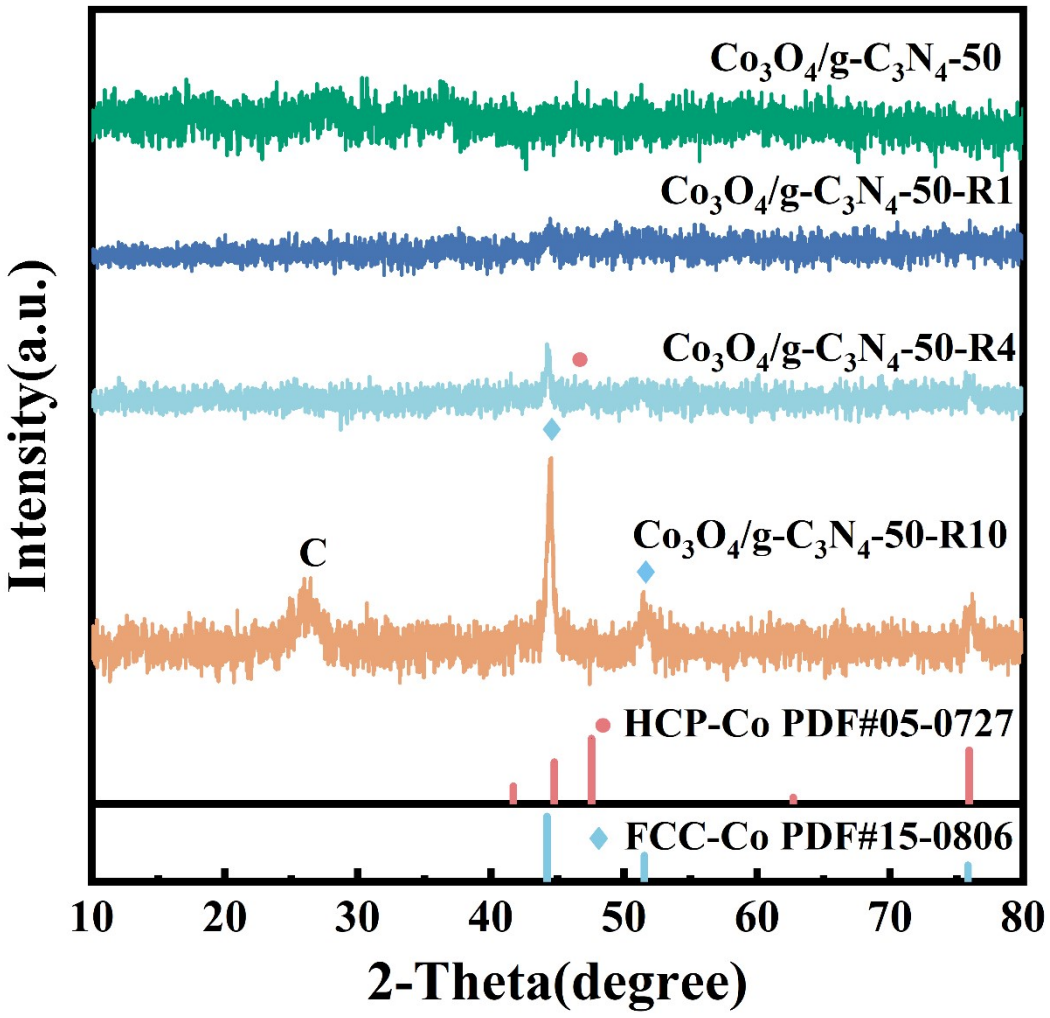

Figure S15. XRD patterns of Co_3O_4/g-C_3N_4-50 after 1 h, 4h and 10 h of reaction.

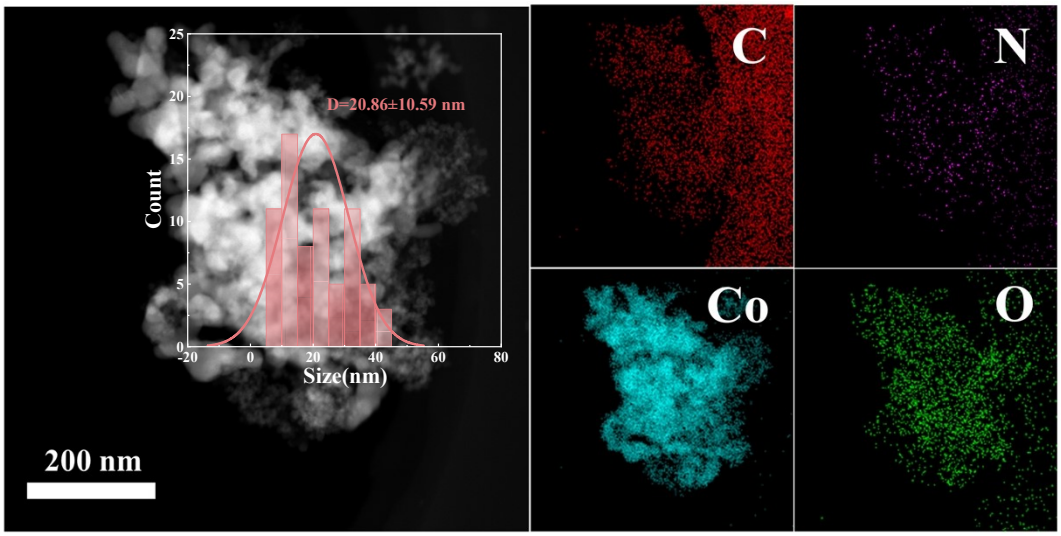

Figure S16. EDS mapping of Co_3O_4/g-C_3N_4-50 after 1 h of reaction.

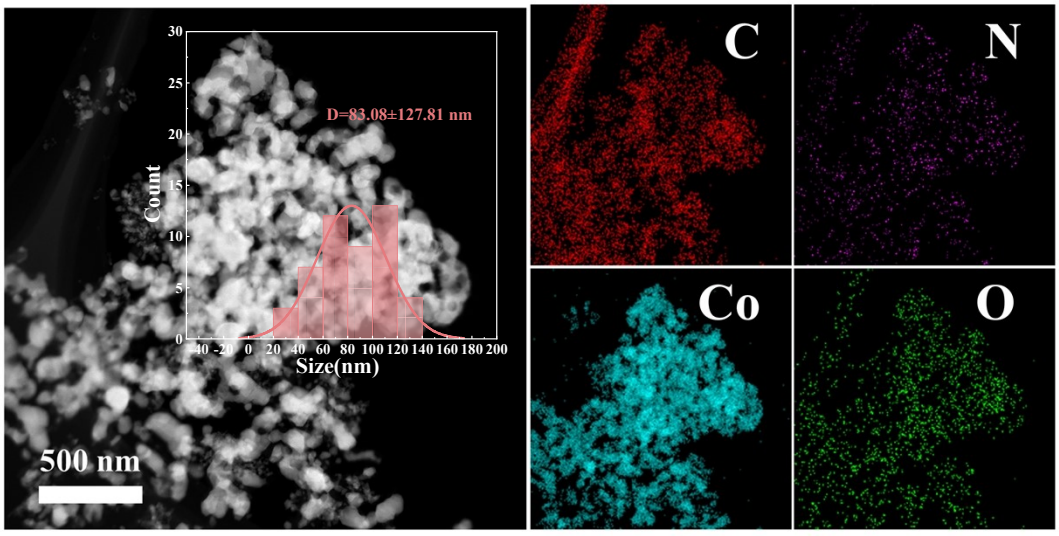

Figure S17. EDS mapping of Co_3O_4/g-C_3N_4-50 after 4 h of reaction.

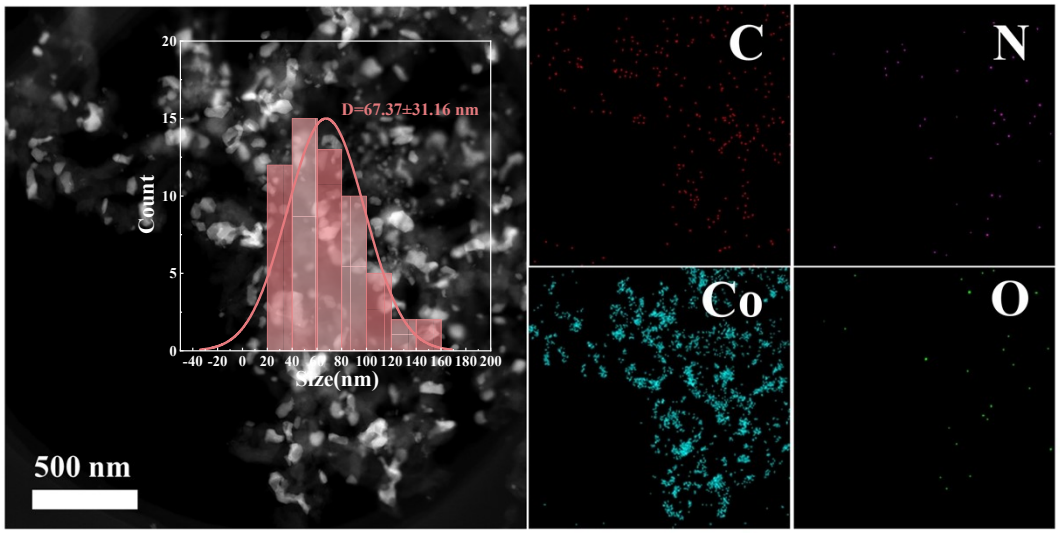

Figure S18. EDS mapping of Co_3O_4/g-C_3N_4-50 after 10 h of reaction.

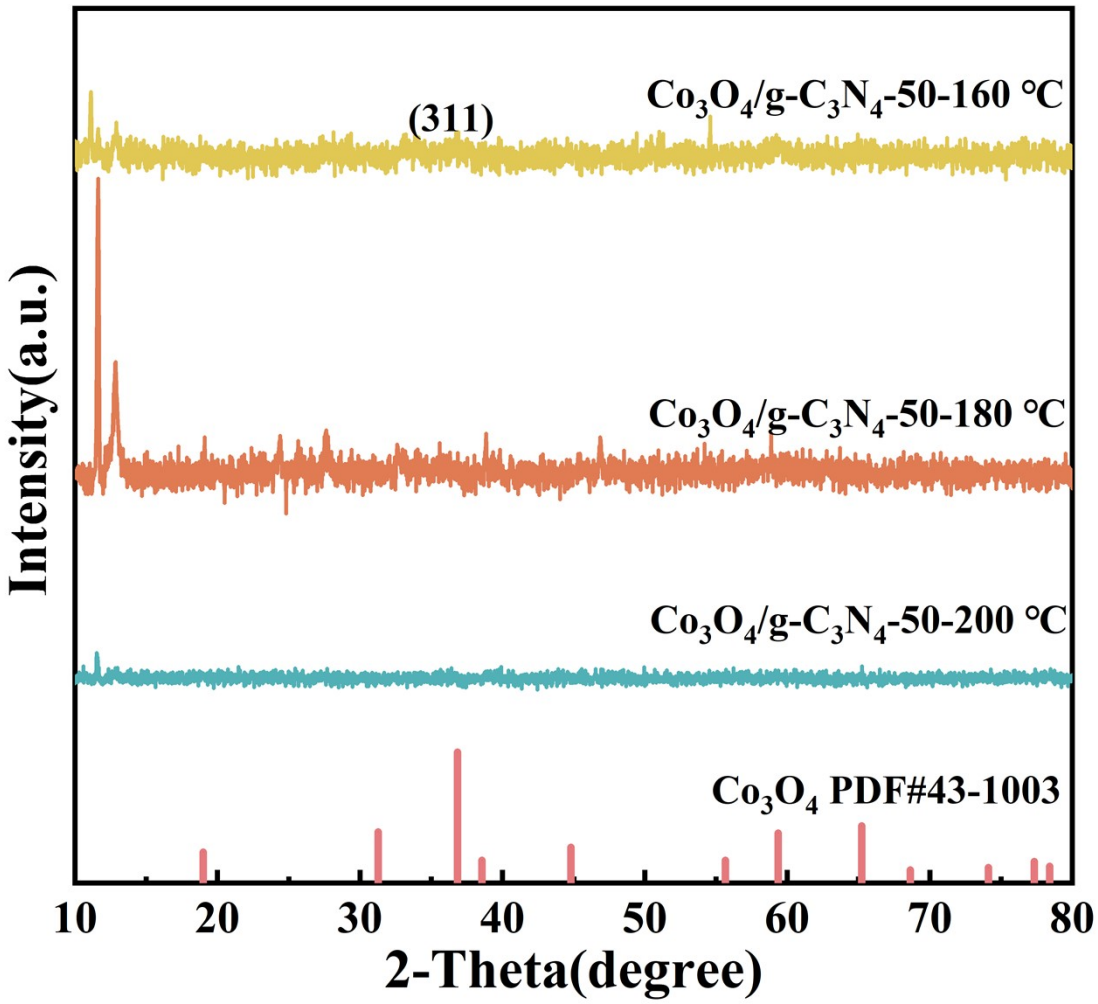

Figure S19. XRD patterns of Co_3O_4/g-C_3N_4-50-160 ℃, Co_3O_4/g-C_3N_4-50-180 ℃ and Co_3O_4/g-C_3N_4-50-200 ℃.

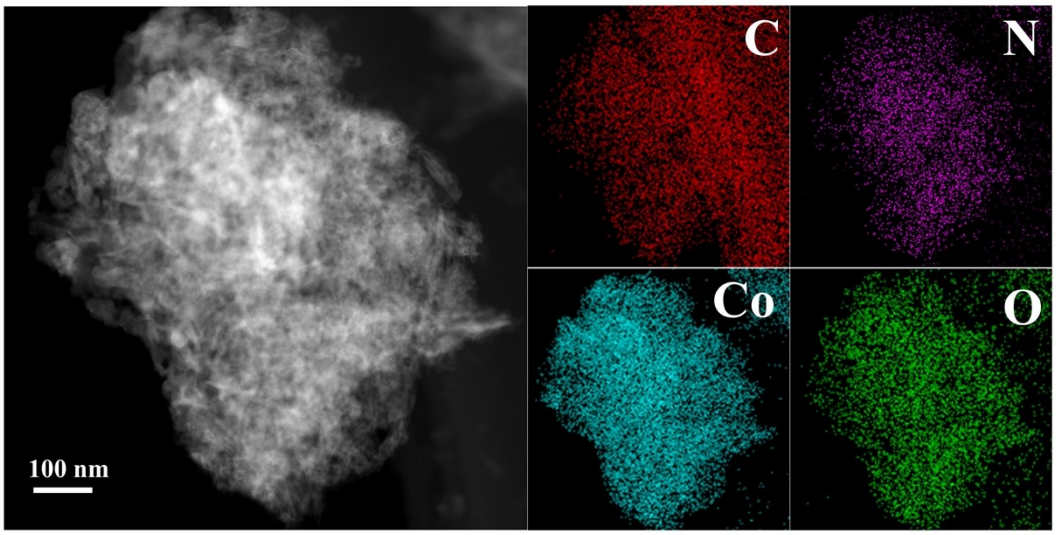

Figure S20. EDS mapping of Co_3O_4/g-C_3N_4-50-180 ℃.

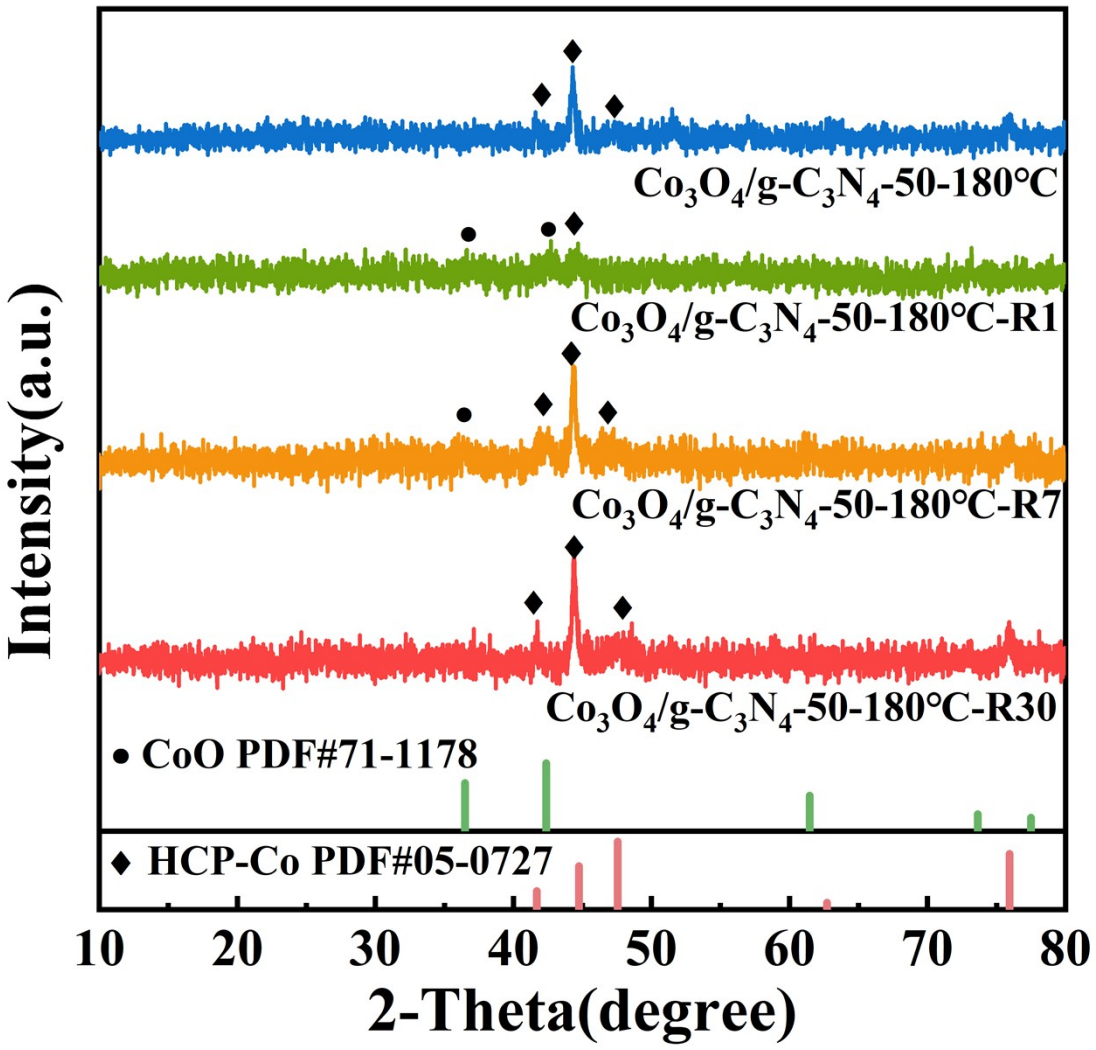

Figure S21. XRD patterns of Co_3O_4/g-C_3N_4-50-180 ℃ after performance evaluation at different temperatures and after the 1 h, 7 h and 30 h stability test at 350 ℃.

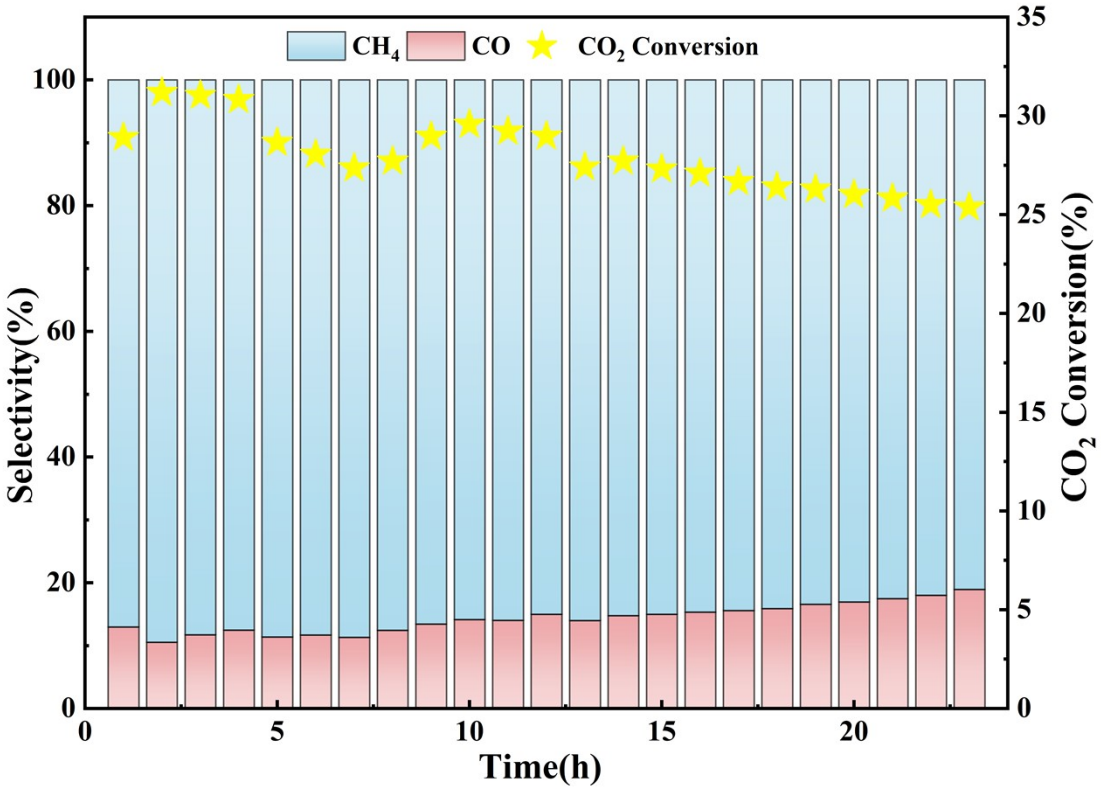

Figure S22. Cycling stability of Co_3O_4/g-C_3N_4-50 180℃ at 380 ℃ over 23 h.

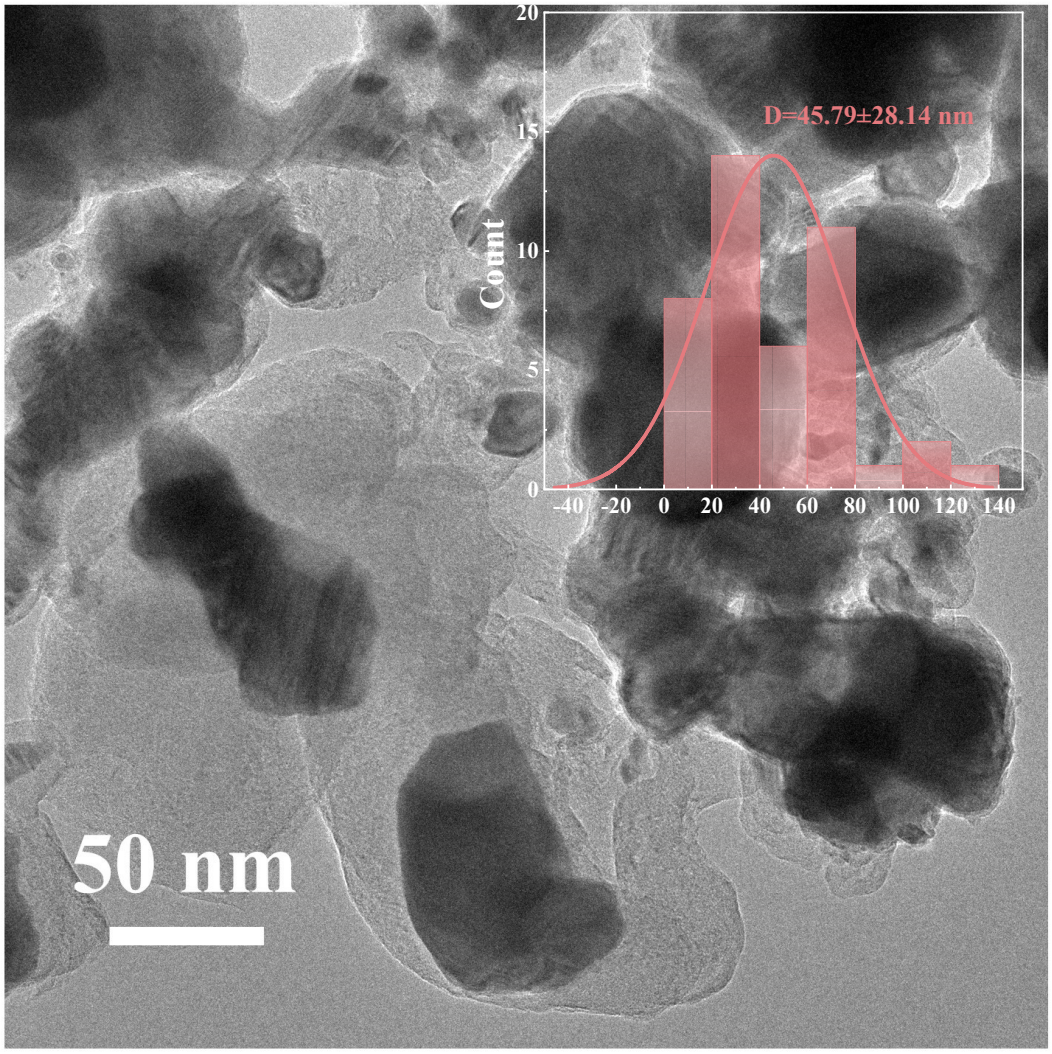

Figure S23. Particle size distribution of Co_3O_4/g-C_3N_4-50-180 ℃ after the cycling stability test.at

Table S1. Electronic structural properties of different catalysts

	Co_3O_4 NPs		Co_3O_4/g-C_3N_4-50		Co_3O_4/g-C_3N_4-50-180 ℃	
	Binding Energy(eV)	Relative(%)	Binding Energy(eV)	Relative(%)	Binding Energy(eV)	Relative(%)
$Co^{3+}(2p^{3/2})$	779.61	49.63	779.46	19.50	779.45	24.23
$Co^{2+}(2p^{3/2})$	781.61	50.37	781.04	80.50	780.6	75.77
O_v	531.11	28.22	531.43	41.93	531.23	26.73
O_{latt}	529.41	64.36	529.72	36.46	529.71	58.06